Soft Matter

Accepted Manuscript

ROYAL SOCIETY OF CHEMISTRY

www.rsc.org/softmatter

Table of Contents Image and text:

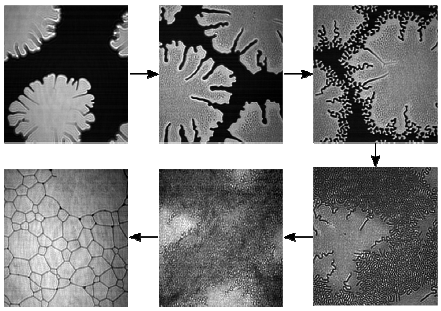

BAM images reveal a sequence of modulated microphases in cluster, stripe, and mosaic morphologies at the liquid-liquid interface.

Microphase formation at a 2D solid-gas phase transition

Adam W. Schuman,* Thomas S. Bsaibes, and Mark L. Schlossman*

Department of Physics, University of Illinois at Chicago, Chicago, IL 60607, USA

Abstract: Density modulated micro-separated phases (microphases) occur at 2D liquid interfaces in the form of alternating regions of high and low density domains. Brewster angle microscopy (BAM) images demonstrate the existence of microphases in cluster, stripe, and mosaic morphologies at the buried interface between hexane and water with fluoro-alkanol surfactant dissolved in the bulk hexane. At high temperature, the surfactant assembles at the interface in a 2D gaseous state. As the system is cooled additional surfactants condense onto the interface, which undergoes a 2D gas-solid phase transition. Microphase structure is observed within a few degrees of this transition in the form of clusters and labyrinthine stripes. Microphases have been observed previously in a number of other systems; nevertheless, we demonstrate that adsorption transitions at the liquid-liquid interface provide a convenient way to observe a full sequence of temperature-dependent 2D phases, from gas to cluster to stripe to mosaic to inverted stripe phases, as well as coexistence between some of these microphases. Cracking and fracture of the clusters reveal that they are a solid microphase. Theories of microphases often predict a single length scale for cluster and stripe phases as a result of the competition between an attractive and a repulsive interaction. Our observation that two characteristic length scales are required to describe clusters whose diameter is much larger than the stripe period, combined with the solid nature of the clusters, suggests that a long-range elastic interaction is relevant. These results complement earlier X-ray measurements on the same system.

*Authors to whom correspondence should be addressed: aschum3@uic.edu, schloss@uic.edu

Introduction

Density modulated phases on the microscale have been observed in a variety of physical systems, including monolayers of insoluble surfactants supported on liquid surfaces.[1-4] Analytical theory and simulations demonstrate that competing interactions, such as a short-range attractive and a long-range repulsive interaction, produce a modulation length scale that is manifest in patterns of clusters or stripes.[2,5,6] In the case of surfactant molecules, the competition is believed to occur between attractive van der Waals forces and longer ranged repulsive dipole-dipole interactions. Theories of microphases in the vicinity of a liquid-vapor critical point, whose domain pattern is driven by either temperature or the surface density of particles, predict a sequence of 2-dimensional (2D) phase transitions from a low density homogeneous 2D gas phase to a cluster phase of condensed liquid-like 2D domains surrounded by gas, then to a liquid-like 2D stripe phase.[7-9] Further increasing the surface density leads to a transition from the stripe phase to an inverse cluster phase where gas domains are surrounded by a liquid-like condensed region, and ultimately to a homogeneous 2D liquid phase at the highest densities. Numerous experimental observations of some aspects of the predicted microphase sequence outlined above have been reported through various methods of driving the phase transition. These include temperature-driven continuous transitions,[10] surface curvature gradient-driven transitions,[11] and film thickness gradient-driven transitions for thin layers of block copolymers.[12]

Here, we demonstrate the formation of density modulated microphases of surfactants at a buried liquid-liquid interface that occurs near a first order transition between interfacial 2D gas and 2D solid phases. Cooling through the first-order

adsorption transition, in which surfactant molecules dissolved in the upper organic bulk liquid solution spontaneously adsorb onto the liquid-liquid interface with the lower phase of bulk water, thus varying the interfacial density of surfactants, allows for the study of a sequence of microphases (Fig. 1). Cluster faceting and fracture that occur in the 2D solid phases are also observed. The system that we study has been previously investigated with a Brewster angle microscope (BAM)[13], though only cluster microphases were reported and they were observed over a wide range (~10 °C) in temperature. These observations were not consistent with X-ray measurements,[14] which prompted this reinvestigation by BAM.

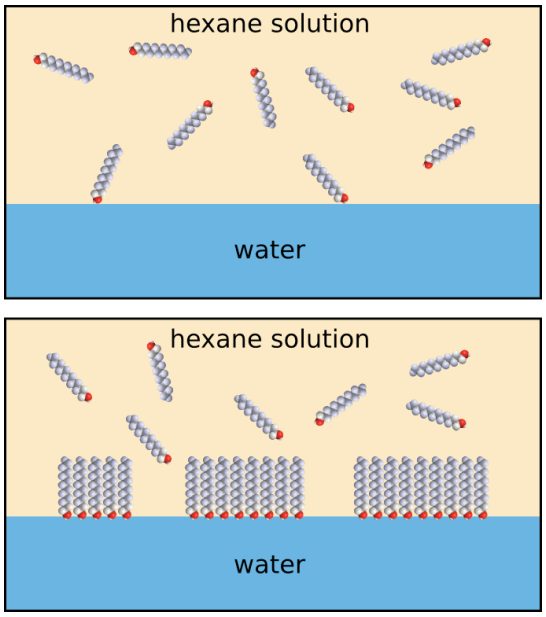

Figure 1 Drawing of a hexane-water interface in cross-section. Top panel - at a temperature above a transition temperature (to be discussed later). Bottom panel - temperature below the transition temperature. Below the transition, surfactants dissolved in the hexane solution self-assemble at the interface into a molecular monolayer in which the polar head group of the surfactant is in contact with water.

Materials and Methods

The bi-phase liquid sample consists of a hexane solution of 1,1,2,2-tetrahydro perfluorododecanol ($CF_3(CF_2)_9(CH_2)_2OH$, denoted FC12OH) at a concentration of 2 mmol/kg placed in contact with pure water. FC12OH molecules can be considered to be rigid cylindrical rods to a first approximation. The FC12OH (> 97%), purchased from Alpha Aesar, is twice recrystallized by slowly cooling a supersaturated solution of FC12OH in hexane. N-hexane from Sigma Aldrich (>99.0%) is purified by filtration through an alumina filled gravity column several times.[15] Water is treated by reverse osmosis and further filtered through a Barnstead Nano-pure UV system. Sample cell cleanliness and material purity are critical for these experiments. Slightly impure samples exhibit lower interfacial tension, a lower transition temperature, clusters that are much larger and less faceted, and absence of the stripe phase.

The sample liquids are contained in a hermetically sealed Teflon coated aluminum cell, which is encased in a cylindrical aluminum thermostat to control the temperature to within 0.01 °C. Prior to measurement, the temperature is raised far above the phase transition to anneal the sample. Then, it is slowly cooled and allowed to equilibrate at each temperature for a duration Δt of at least an hour while the bottom phase is gently stirred until temperature variations are within 0.03 °C over a period of 20 minutes. Measurements are taken subsequently with the stirring turned off.

The sample cell and optical setup shown in Figure 2 allow for sequential Brewster angle microscopy to image surfactant domains and quasi-elastic light scattering (QELS) to measure interfacial tension.[13,16,17] The reflection of *p*-polarized light at the Brewster angle would be extinguished from an ideal, step-function dielectric interface, but

deviations from ideality due to the presence, *e.g.*, of monolayer domains, lead to weak reflections that are used to image the interfacial phase morphology. Since the camera is at an oblique angle to the interface, only a fraction of the total field of view is in focus at one time. To account for this, 10 to 50 images are captured while the focus is scanned across the surface. The images are digitally pieced together in imageJ software for a single composite in-focus image. The image is electronically stretched to the surface's true aspect ratio to correct for the distorted aspect ratio from the camera's oblique viewing angle. For visual clarity, each image is separately contrast enhanced by linearly scaling the histogram of captured pixel values to span the full range of possible pixel values. Images are recorded at one of two magnifications – 17.4x and 3x – with a horizontal field of view of 380 μm and 2.25 mm, respectively. The 3x images occasionally exhibit narrow horizontal bands along the top edge as a result of optical interference from the microscope and should not be regarded as part of the liquid surface structure. The 3x images additionally exhibit a pronounced gradient of laser illumination with enhanced brightness in the image center that represents the shape of the laser beam.

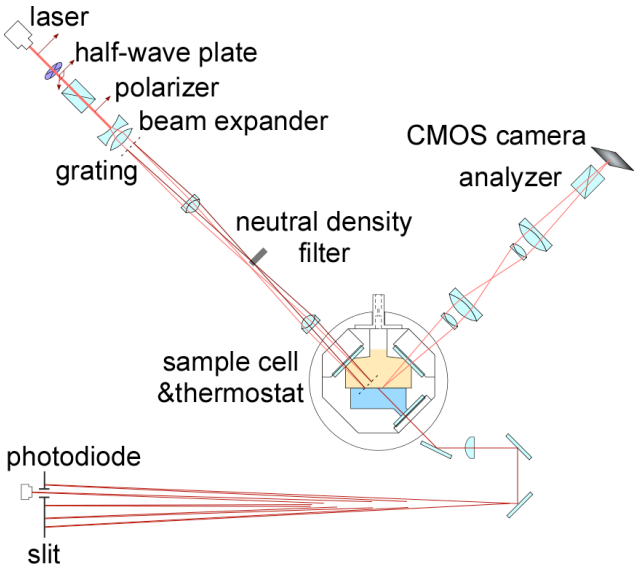

Figure 2 Brewster angle microscope (BAM) with quasi-elastic light scattering (QELS) setup. The sample cell has three glass windows: a window for the incident in-plane polarized Coherent Compass 315M Nd-YAG 532 nm laser at the Brewster angle, a window for the reflected image of the interface to be recorded by a Mightex MCE-B013-UW CMOS camera, and a window for light transmitted through the interface to be recorded by a photodiode for QELS measurement. The camera exposure is adjusted by changing the shutter speed for each magnification of the focusing optics. An analyzer is installed directly before the camera to reveal surface anisotropy. When QELS measurements are made, a beam expander, grating, neutral density filter and neighboring achromatic doublet lenses are placed between the sample cell and the incident laser to image the external grating onto the interface. The grating acts as a local oscillator for heterodyne detection, part of the QELS technique. These additional components are swapped out for BAM imaging.

Results and Discussion

Figure 3 shows the variation of interfacial tension with temperature. A discontinuity in the slope of the tension signals the location of a first order phase transition.[18] Two straight-line fits to the interfacial tension, one above and one below the phase transition temperature, intersect at $T_o = 41.17$ °C. This temperature coincides with the point where interfacial cluster domains first become visible (Fig. 3B). At temperatures slightly below T_o, the cluster phase as a whole flows slowly across the

microscope field of view at a speed of approximately 5 micrometers per second, possibly due to convective motion of the liquid-liquid interface, but the separation between neighboring clusters remains essentially constant. This motion stops at a temperature further below T_o as a result of the growth of the stripe phase that produces nearly full coverage of modulated surfactant density across the entire liquid-liquid interface (Fig. 3E). This corresponds to a sharp change in interfacial tension as shown in the inset of Fig. 3 by a kink in the tension data appearing slightly below T_o (indicated by the arrow in the inset). The interfacial tension of FC12OH+hexane-water system is reproducible upon cooling and heating, except that the kink slightly below T_o is not observed upon heating. This was confirmed for multiple trials on the same prepared sample, and for newly prepared samples.

X-ray reflectivity and off-specular diffuse scattering measurements of this system have previously demonstrated that above T_o, the interface is essentially a pure water-hexane interface, though there may be a very low concentration of FC12OH molecules at the interface (referred to as a gaseous monolayer of FC12OH).[14,19,20] Several degrees below T_o the interface is nearly fully covered by a 12.4 ± 0.3 Å thick monolayer of molecules with electron density measured to be 0.633 ± 0.013 e^- $Å^{-3}$. These are the expected values for an X-ray reflectivity measurement of a monolayer of FC12OH molecules oriented normal to the interface and packed in an arrangement similar to solid 3D fluoroalkanes in either a crystalline or a rotator solid phase (note that the X-ray reflection is dominated by the fluorocarbon part of FC12OH).[21] Liquid phases of fluoroalkanes are ~20% less dense and could have been easily distinguished from the solid phase by X-ray measurements.[19,21,22] Earlier X-ray reflectivity and off-specular

diffuse scattering measurements indicated that the interface is partially covered by monolayer domains of FC12OH molecules within 2 to 3 °C of T_o.[14,19,20]

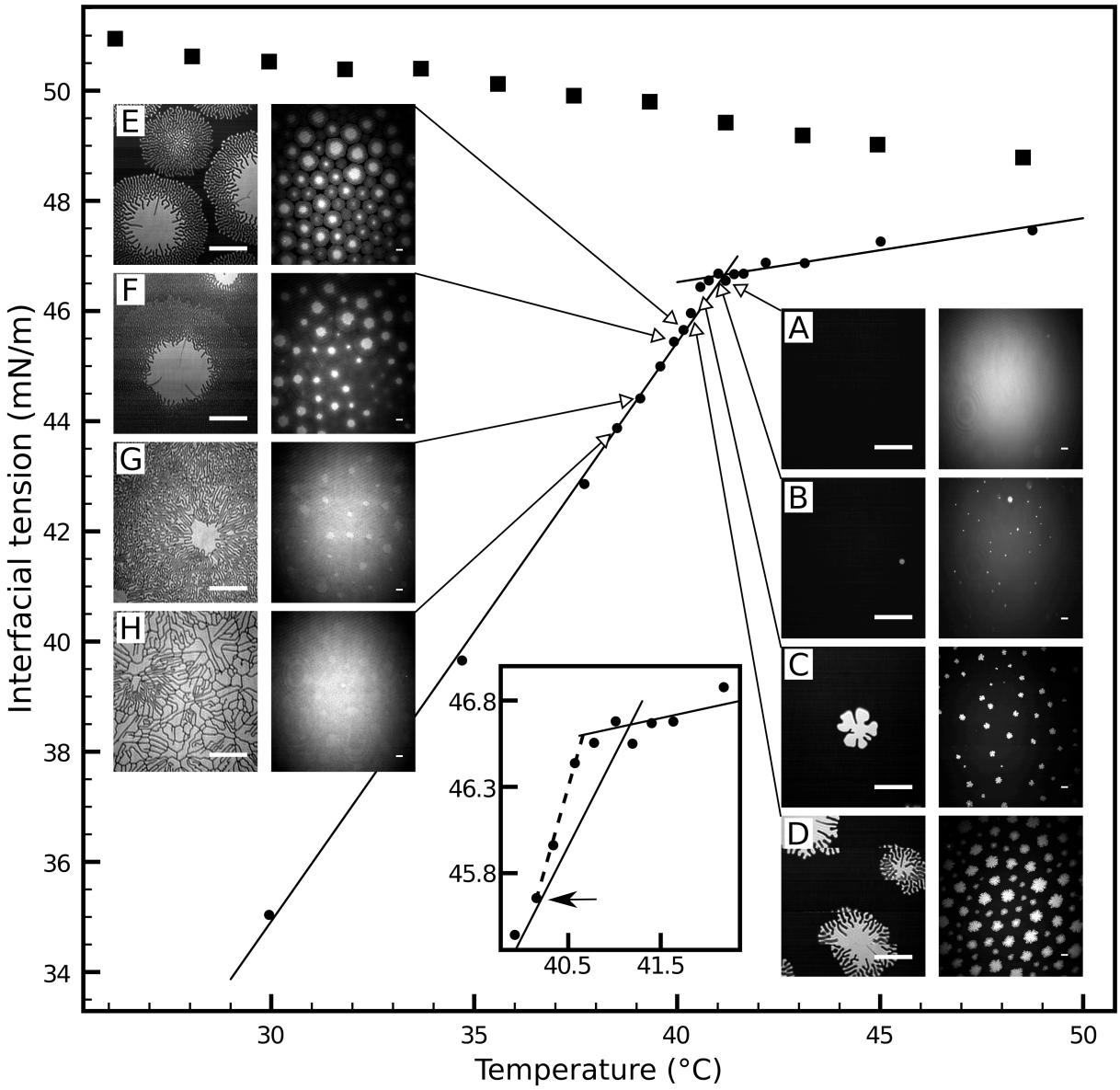

Figure 3 QELS interfacial tension and BAM images for pure hexane-water (squares) and for 2 mmol/kg FC12OH + hexane-water (solid dots) with an average error of 0.05 mN/m. The solid lines represent linear fits. The inset at bottom center shows the interfacial tension data near the transition, where the arrow indicates the location of the change in slope, described in the text, which corresponds to the formation of nearly full coverage of microphases across the interface. The dashed line is a visual guide. Brewster angle microscope images are taken *in situ* for each data point at two separate magnifications.

Within each image pair, the left image is at 17.4x magnification and the right is at 3x magnification with a horizontal field of view of 380 μm and 2.25 mm respectively. The 3x images exhibit a pronounced gradient of laser illumination with enhanced brightness in the image center that represents the shape of the laser beam. Scale bars represent 100 μm. Equilibration time Δt in h: (A) 1.5 (B) 16 (C) 1.5 (D) 1 (E) 1.5 (F) 2 (G) 6 (H) 38. Total time t_d (in hours) since the first appearance of domains: (A) -16 (B) 0 (C) 3.5 (D) 4.5 (E) 6 (F) 8 (G) 35.5 (H) 74.

Figure 3 displays selected BAM images during sample cooling through the phase transition. Figure 3A is a typical nearly black image just above T_o that reveals a lack of structure, consistent with the X-ray observations of a gaseous phase above the transition. Cluster domains with diameters of around 10 μm appear suddenly (Fig. 3B), within a single 0.2 °C cooling step from Fig. 3A. Figure 3C indicates that the size of each cluster grows with an increasingly more irregular shape as the temperature is decreased. Dendritic growth appears on the cluster periphery at $T - T_o \approx -0.8\,°C$ (Fig. 3D). Cluster-stripe coexistence appears upon incrementally lowering the temperature further, causing the dendritic legs to thin and lengthen (Fig. 3E) until the region surrounding the clusters is consumed by a stripe phase (Fig. 3F). The decrease in size and number of the cluster domains suggests that the newly formed dendritic legs are redistributing surfactant from the cluster centers to the surrounding stripe phase, though additional surfactant is adsorbed to the interface as the temperature is lowered to further populate the stripe phase. Further reduction of the temperature leads to modifications in the stripe phase (Fig. 3G) until the surface is completely covered in a homogeneous mosaic (Fig. 3H) where polydispersed regions of 2D solid are delimited by crack-like stripes.

The initial size of newly formed clusters as well as the maximum interfacial coverage of the clusters prior to transitioning into the stripe phase depends on the temperature quench depth below T_o, as well as the size of subsequent temperature steps.

When the temperature is dropped by slightly less than 0.2 °C below T_o, the cluster domains first become visible with a diameter of about 20 μm at a total interfacial coverage of 0.2%, similar to Fig. 3B. Subsequent cooling with a step size of 0.05 °C between measurements leads these clusters to sprout dendrites (Fig. 4A, B, C) that form a stripe phase almost completely free of any cluster domains (Fig. 4D, E). The sequence in Fig. 3 undergoes a similar quench depth of 0.16 °C but with a larger temperature step of 0.2 °C that leads to a higher cluster coverage. The irregularity in cluster shape upon cooling is demonstrated through the sequence of images in figure 4A.

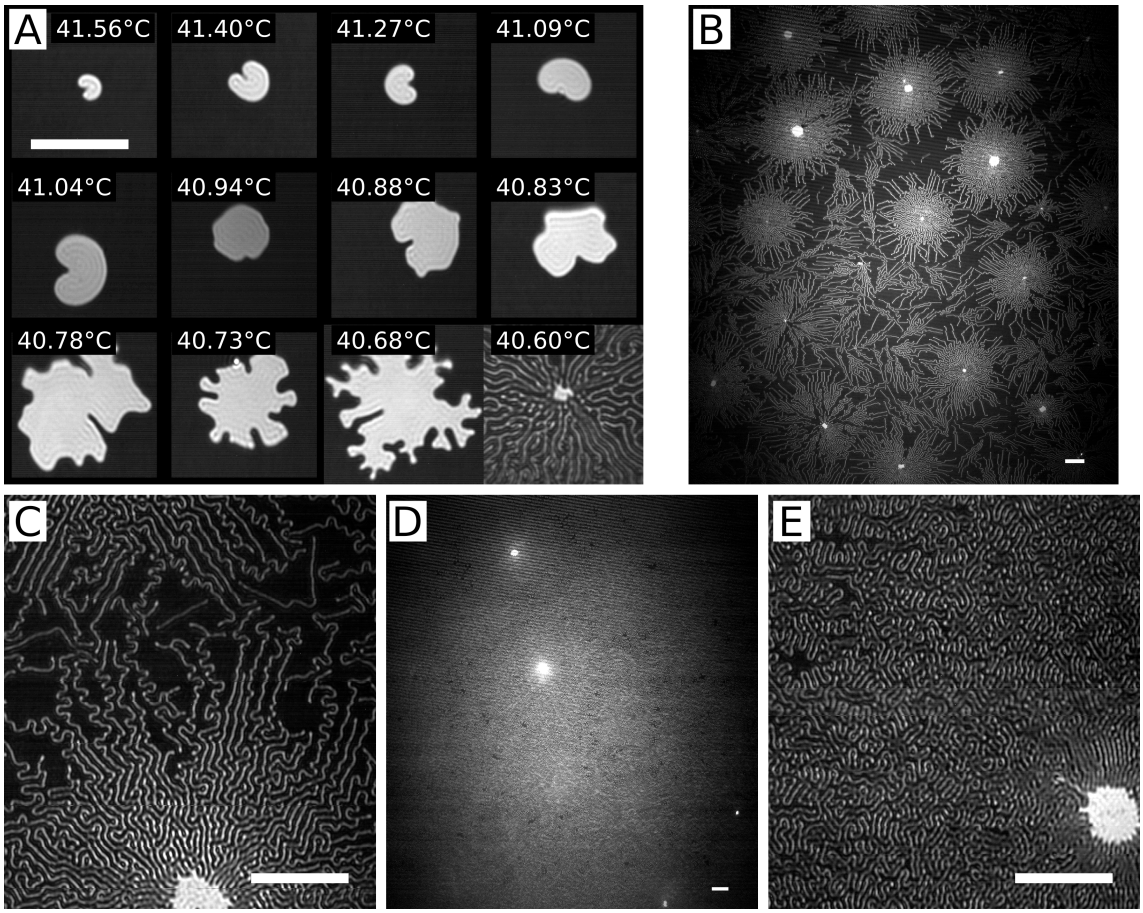

Figure 4 BAM images of a cooling sequence of FC12OH surfactant microphases at the water-hexane interface. Images in A show a cluster domain at each temperature up to the start of the stripe phase. The transition temperature could not be determined precisely from the surface tension data, therefore temperature is listed in °C: (B) 40.57, (C) 40.52

(D & E) 40.42. The white scale bars represent 100 μm. Total time t_d (in hours) since the first appearance of domains: (A) top row (left to right): 0, 1, 4.5, 22.5; middle row: 42.5, 44, 45.5, 46.5; bottom row: 48, 49, 50.5, 68.5 (B) 70 (C) 72.5 (D & E) 76. Equilibration time Δt in h: (A) top row (left to right): 2, 1, 3, 18; middle row: 20, 1.5, 1.5, 1; bottom row: 1.5, 1, 1.5, 18 (B) 1.5 (C) 1.5 (D & E) 1.5.

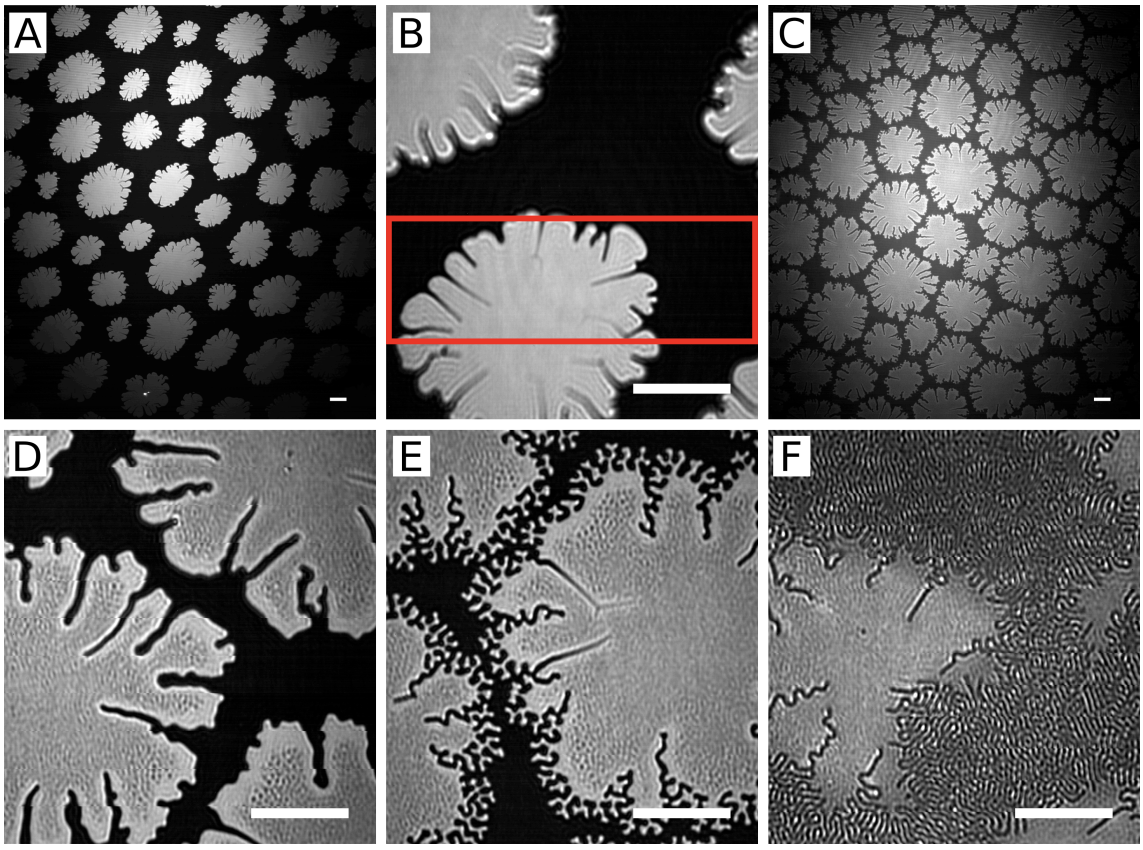

Figure 5 BAM images of a cooling sequence of FC12OH surfactant microphases at the water-hexane interface formed at a quench depth of 0.73 °C. Due to a surface drift, panel B could not be imaged as an assembly of in-focus images but is, instead, a single snapshot where the in-focus region is indicated by a red bounding box. $T_o = 41.2$ °C. Temperature in units of $T - T_o$ (°C): (A & B) -0.7, (C & D) -1.2, (E) -1.4, (F) -1.5. The white bars represent 100 μm. Total time t_d (in hours) since the first appearance of domains: (A & B) 0 (C & D) 19.5 (E) 20.5 (F) 42.5. Equilibration time Δt in h: (A & B) 1 (C & D) 1 (E) 1 (F) 22.

Figure 5 shows the formation of large cluster domains with high interfacial coverage when the quench depth is 0.73 °C below T_o, which is larger than the quench

depths for Figs. 3 and 4. The cluster formation in Fig. 5A,B is measured directly at the quench depth and exhibits an average cluster diameter of 240 μm and a total interfacial coverage of 40%. Figure 5C,D are measured at the lowest temperature prior to stripe formation at which the cluster size reaches a maximum with an average diameter of 260 μm and a total interfacial coverage of 70%. Cluster domains do not make direct contact with one another even at high coverage, but assemble loosely into a hexagonal lattice. This may be the result of repulsive long-range electrostatic dipole-dipole interactions between the surfactants. The cluster periphery sprouts dendritic fingers in Fig. 5E. The mottling in the interior of the cluster domains in panels D and E of Fig. 5 may be reminiscent of incipient stripe formation, but as shown in figure 5E, stripe domains form by fingering along the cluster perimeter where there is a dense uniform band absent of any internal structure. We have not observed stripes evolving from the cluster interior. Large clusters coexist with the stripe phase at slightly lower temperature (Fig. 5F). The persistence of clusters to low temperatures, in comparison to Fig. 4, is related to the larger temperature quench depth. Regardless of the quench depth, the same morphological sequence of phases is always observed: gas to clusters to stripes to mosaic solid.

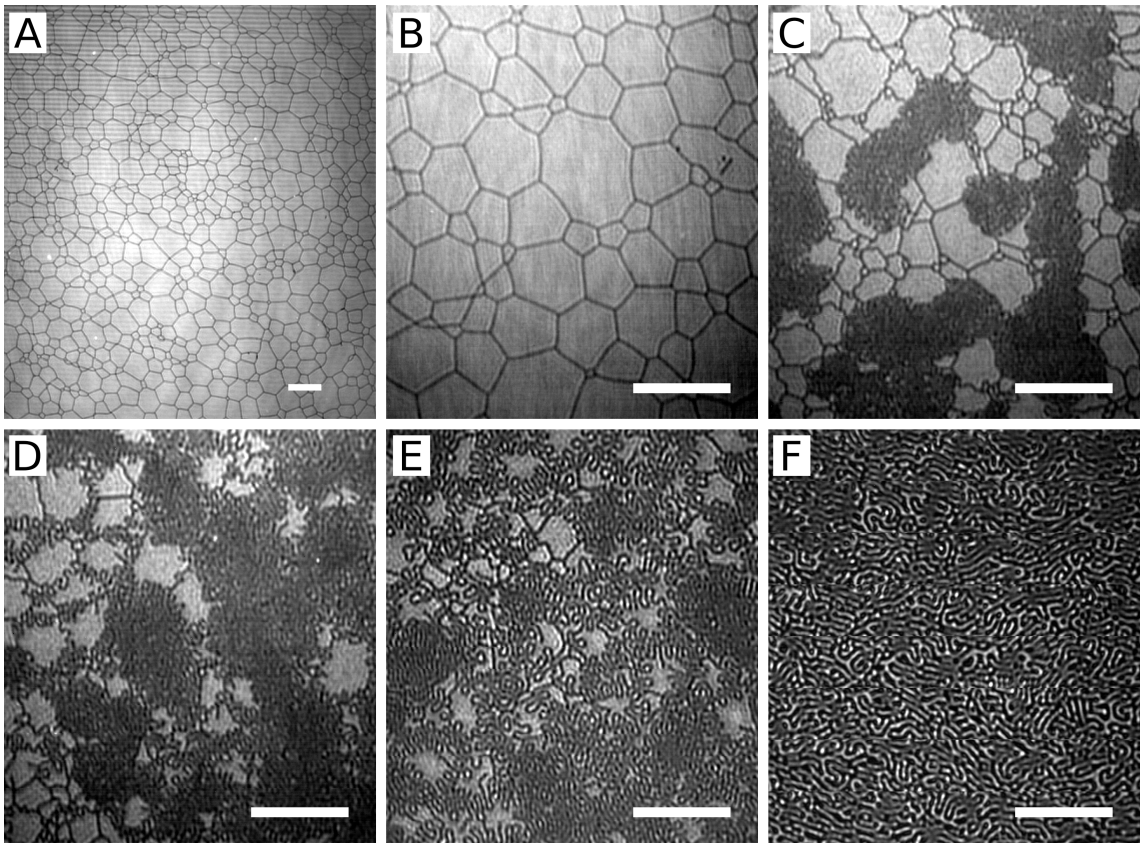

Figure 6 BAM images of a heating sequence of FC12OH surfactant microphases at the water-hexane interface. $T_o = 40.5$ °C. Temperature in units of $T - T_o$ (°C): (A & B) -3.0, (C) -2.1, (D) -1.4, (E) -0.9, (F) -0.7. The white bars represent 100 μm. Time of measurement relative to panel A in h: (A & B) 0 (C) 18 (D) 21 (E) 24 (F) 40.5. Equilibration time Δt in h: (A & B) 1.5 (C) 18 (D) 1 (E) 3 (F) 1.5.

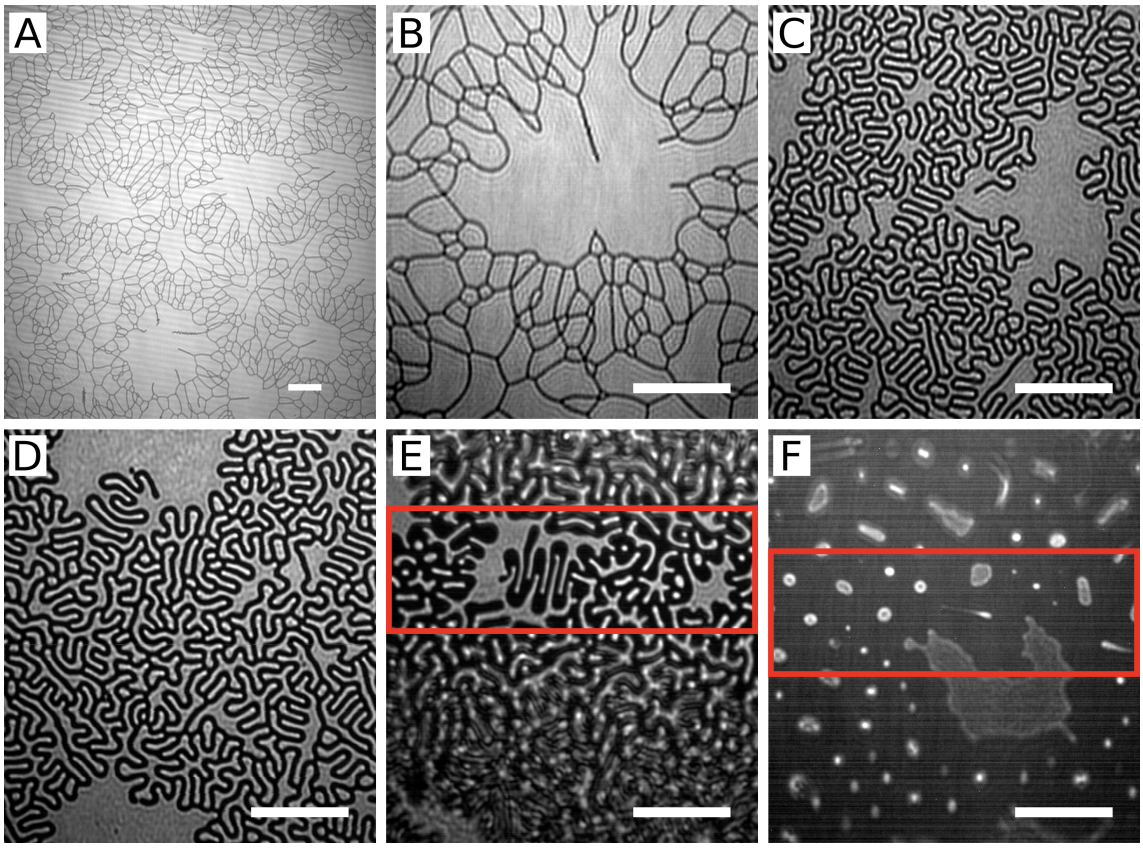

Figure 7 BAM images of a heating sequence of FC12OH surfactant microphases at the water-hexane interface. Due to a surface drift, panels E and F could not be imaged as an assembly of in-focus images but consist of a single snapshot where the in-focus region is indicated by a red bounding box. $T_o = 41.2$ °C. Temperature in units of $T - T_o$ (°C): (A & B) -1.6, (C) -0.7, (D) -0.5, (E) -0.2, (F) 0.0. The white bars represent 100 μm. Time of measurement relative to panel A in h: (A & B) 0 (C) 18 (D) 19 (E) 20 (F) 39.5. Equilibration time Δt in h: (A & B) 1 (C) 18 (D) 1 (E) 1 (F) 19.5.

Upon heating the sample, the interfacial tension is repeatable and an inverted stripe phase appears (Figs. 6, 7). Although the stripe period of the inverted stripe and stripe phases are similar, *e.g.*, 6 μm in Figs. 4E and 5F, 7 μm in Fig. 6F and 9 μm in Fig. 7C, the inverted stripe morphology consists of low density stripes within a high density background (most clearly exhibited in Figs. 7C-D). Additionally, the stripes formed upon heating tend to persist at temperatures closer to T_o than where they first appeared

upon cooling. The width of inverted stripes generally increase with temperature (e.g., Fig. 7C to D to E) and, in one set of images, we observed that the shape of inverted stripes changes to increase the width in regions of high curvature (Fig. 7E). The overall features are consistent with a reduction of surfactant interfacial density as expected for increasing temperature.

Variable results upon heating are attributed to the initial condition of the mosaic phase that, in turn, is dependent on the cooling history directly prior to heating. The evolution of the stripe phase in Fig. 6 shows coexistence of the stripes with the mosaic structures formed at low temperature (Figs. 6B-E). This system eventually progresses to a uniform stripe phase (Fig. 6F). Figure 7 shows the stripe phase forming at higher temperature and coexisting with cluster domains through the entire temperature duration of the stripe phase. The system in Fig. 7 was heated directly after the series of measurements shown in Fig. 3 where cluster domains persist through the entire duration of the cooling process. The cooling process prior to Fig. 6 formed a stripe phase free of clusters similar to Figure 4. The presence of the cluster domains affects the shape of the mosaic phase (Figs. 6A-B, 7A-B) and may cause the variations observed upon heating.

The stabilization of cluster domains that are more than an order of magnitude larger than the stripe phase is unexpected and suggests the importance of an additional very long-range interaction, which may be the result of the solid nature of the clusters. Figure 8 shows a domain that has fractured into two pieces, thus providing evidence that the cluster domain interior is solid. In addition, the optical reflectivity of the clusters is relatively high, consistent with results of earlier X-ray measurements that the molecules are densely packed into a 2D solid phase.[14,20] Clusters grow with a homogeneous central

core beyond which radial defects appear. For example, Fig. 5 shows clusters that exhibit radial defects extending 50 to 100 μm from their perimeter. The defects may arise as a result of lattice strain that develops as the cluster grows. The faceted edges of the defects, for example in Figs. 5B, 5E, additionally show that the domain interior is solid-like, at least near the center of the domains. The periphery, on the other hand, is often rounded, which may indicate that the 2D facets are roughened[23] (Figs. 5A-B). Once the clusters sprout dendritic fingers at lower temperature, the internal defects roughen into undulating paths near the domain edge (Fig. 5E).

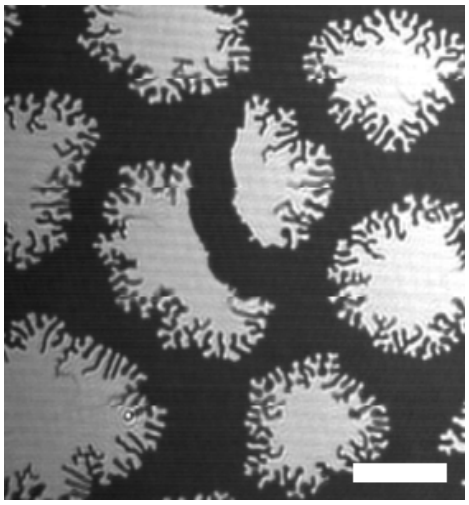

Figure 8 Section of a BAM image showing a cracked cluster domain. T_o = 40.6 °C. Temperature in units of $T - T_o$: -0.6 °C. The white bar represents 100 μm. Total time t_d since the first appearance of domains is 1 hour. Equilibration time Δt = 1 h.

Several aspects of our measurements indicate that kinetics play a role in our observations, in spite of our efforts to fully equilibrate the interface before every measurement. For example, the Gibbs phase rule applied to this system indicates that coexistence of two interfacial phases should occur at only one temperature for a chosen bulk pressure and surfactant concentration[24,25] yet we have observed the persistence of cluster/stripe coexistence (Figs. 3 & 4) and mosaic/inverted-stripe coexistence (Fig. 6)

over a range of one to two degrees. Our observations that the size of clusters depends upon both the initial quench depth through the transition and the size of subsequent temperature steps further illustrates the role of kinetics. Clusters are smaller for smaller quench depths and temperature steps, though even the smallest temperature quenches (of ~ 0.1 °C) and steps (of 0.05 °C) produce clusters, as in Fig. 4A, which undergo a subsequent transition to the stripe phase. The appearance of a stripe phase upon cooling through the adsorption transition is always preceded by a cluster phase. Experimental observations reveal that clusters are stable for up to 48 h yet their absence in the sequence of phases observed upon heating may indicate that they are a long-lived metastable state. Further experiments are required to explore this issue.

Several aspects of the BAM observations agree with earlier X-ray scattering studies of this system. The stripe phase measured directly from BAM images and its Fourier transform at $T - T_o \approx -0.6$ °C have a period of 6 μm, consistent with the domain spacing measured by X-ray off-specular diffuse scattering.[14] The BAM imagery further clarifies that at this temperature, the domain morphology consists of labyrinthine stripes. The entire structural transition from homogeneous 2D gas to 2D solid occurs within 2 to 3 degrees of T_o, also in agreement with X-ray data.[14] Placing an optical polarizer (the analyzer in Fig. 2) before the camera did not reveal anisotropy for any polarizer rotation angle, thus indicating that organized regions of molecules tilted with respect to the interfacial normal are not present. This is true for all BAM images and is consistent with the result from X-ray reflectivity that the FC12OH molecules are oriented normal to the interface.[19]

Our observations of a sequence of gas to cluster to stripe phases are qualitatively consistent with a theory of a single component 2D fluid, which interacts via short-ranged attractive and long-ranged repulsive interactions, in the vicinity of a liquid-gas critical point.[3,9] These BAM observations, however, are measured from a sample near a 2D solid-gas transition. Well below the phase transition temperature, the mosaic phase exhibits faceted domains, similar to solid 2D crystals, as previously observed in another measurement of a 2D Gibbs monolayer.[26] Such observations, among others discussed in this paper, cannot be predicted by a theory of 2D fluids. Perhaps an alternative phase diagram of a system with competing short and long-range interactions would be more relevant, such as the one presented by Pini *et al.*, which shows a liquid-gas transition preempted by a fluid-solid transition.[27] This theory is, however, calculated for a range of interactions that do not produce microphases and additional theory is required to show the existence of microphases near a fluid-solid transition.

To our knowledge, the presence of clusters with an average diameter many times larger than the stripe period has not been predicted theoretically. In addition, most experimental observations of cluster-stripe coexistence exhibit clusters and stripes of similar dimension.[10-12,28-30] We are aware of one observation of cluster-stripe coexistence with different size clusters and stripes, recorded by atomic force microscopy of a Langmuir lipid monolayer transferred to a mica surface, which revealed the cluster radius to be about four times larger than the stripe width.[31] The observations presented here show a much larger difference in size, with clusters of diameter ~40 times larger than the stripe period.

Conclusion

In summary, soluble rigid rod surfactants adsorbed onto a liquid-liquid interface form microphase domains that appear with the onset of a first order adsorption transition. The 2D gas-solid transitions include a full sequence of microphases including 2D cluster, 2D cluster-stripe coexistence, 2D stripe and a 2D mosaic phase, which, upon heating, is converted to a coexistence of 2D mosaic and inverted stripe phase, and ultimately to a 2D inverted stripe phase. The characteristic length scale of these microphases are not all the same, as expected for liquid-like 2D microphases that appear near a 2D liquid-vapor critical point.[3,9] Instead, 2D solid clusters are observed whose size depends upon the temperature quench depth through the transition. The initial cluster size influences subsequent phases, including the temperature range for stripe/cluster coexistence and the morphology of the mosaic and inverted stripe phases. Clusters on the order of ~250 μm have been observed that can be compared to the stripe period of 6 μm. Large clusters have a homogeneous central core with a diameter up to about 50 to 100 μm, beyond which radial cracks appear, thus suggesting the presence of long-range elastic forces that compete with other interactions to stabilize the domain morphology. Although only microphase observations of FC12OH in hexane over water are presented here, adsorption transitions at the interface between organic surfactant solutions and water have been observed by interfacial tension and X-ray measurements for many other chemical systems.[32,33] Future studies are planned for the investigation of flexible and charged surfactant systems that may display qualitatively different behavior.

Acknowledgments

MLS acknowledges support from NSF award CHE-0910825. AWS acknowledges support of a GAANN fellowship from NSF. The assistance of Sai Venkatesh Pingali, Wilson Barajas, and Enas Abu Naser in the construction of an earlier version of the BAM is gratefully acknowledged as is the assistance of Robert Helegda in modification of the BAM.

References

1. M. Seul and D. Andelman, *Science*, 1995, **267**, 476.
2. D. Andelman and R. Rosensweig, *J. Phys. Chem. B*, 2008, **113**, 3785–3798.
3. D. Andelman, F. Broçhard, and J. Joanny, *J. Chem. Phys.*, 1987, **86**, 3673.
4. H. M. McConnell, *Annu. Rev. Phys. Chem.*, 1991, **42**, 171–195.
5. V. I. Marchenko, *Soviet Physics JETP*, 1986, **63**, 1315–1318.
6. A. Archer and N. Wilding, *Phys. Rev. E*, 2007, **76**, 031501.
7. C. O. Reichhardt, C. Reichhardt, and A. R. Bishop, *Phys. Rev. E*, 2010, **82**, 041502.
8. A. Imperio and L. Reatto, *J. Chem. Phys.*, 2006, **124**, 164712.
9. A. Archer, *Phys. Rev. E*, 2008, **78**, 031402.
10. H. Mohwald, *Reports on Progress in Physics*, 1993, **56**, 653.
11. Y. Kaizuka and J. T. Groves, *New J. Phys.*, 2010, **12**, 095001.
12. A. P. Smith, J. F. Douglas, E. J. Amis, and A. Karim, *Langmuir*, 2007, **23**, 12380–12387.
13. S. Uredat and G. Findenegg, *Langmuir*, 1999, **15**, 1108–1114.
14. M. Li, A. Tikhonov, and M. Schlossman, *EPL (Europhysics Letters)*, 2002, **58**, 80.
15. A. Goebel and K. Lunkenheimer, *Langmuir*, 1997, **13**, 369–372.
16. D. Langevin, Ed., *Light Scattering by Liquid Surfaces and Complementary Techniques*, Marcel Dekker Inc., New York, 1992, vol. 41.
17. S. M. Danauskas, M. K. Ratajczak, Y. Ishitsuka, J. Gebhardt, D. Schultz, M. Meron, B. Lin, and K. Y. C. Lee, *Review of scientific instruments*, 2007, **78**, 103705.
18. Y. Hayami, A. Uemura, N. Ikeda, M. Aratono, and K. Motomura, *Journal of Colloid And Interface Science*, 1995, **172**, 142–146.
19. Z. Zhang, D. M. Mitrinovic, S. M. Williams, Z. Huang, and M. L. Schlossman, *J. Chem. Phys.*, 1999, **110**, 7421–7432.
20. A. M. Tikhonov, M. Li, and M. L. Schlossman, *J. Phys. Chem. B*, 2001, **105**, 8065–8068.
21. H. Schwickert, G. Strobl, and M. Kimmig, *J. Chem. Phys.*, 1991, **95**, 2800.
22. H. W. Starkweather, *Macromolecules*, 1986, **19**, 1131–1134.
23. P. M. Chaikin and T. C. Lubensky, *Principles of Condensed Matter Physics*, Cambridge University Press, Cambridge, United Kingdom, 1995.
24. A. M. Tikhonov, S. V. Pingali, and M. L. Schlossman, *J. Chem. Phys.*, 2004, **120**, 11822.
25. R. Defay, I. Prigogine, and A. Bellemans, *Surface Tension and Adsorption*, Longmans, Green & Co. Ltd, London, 1966.
26. B. Berge, L. Faucheux, K. Schwab, and A. Libchaber, *Nature*, 1991, **350**, 322–324.
27. D. Pini, A. Parola, and L. Reatto, *J. Phys.: Condens. Matter*, 2006, **18**, S2305–S2320.
28. R. Plass, J. A. Last, N. C. Bartelt, and G. L. Kellogg, *Nature*, 2001, **412**, 875–875.
29. S. Rozovsky, Y. Kaizuka, and J. Groves, *Journal of the American Chemical Society*, 2005, **127**, 36–37.
30. R. J. El-Khouri, S. L. Frey, A. W. Szmodis, E. Hall, K. J. Kauffman, T. E. Patten,

K. Y. C. Lee, and A. N. Parikh, *Langmuir*, 2011, **27**, 1900–1906.
31. L. K. Nielsen, T. Bjørnholm, and O. G. Mouritsen, *Langmuir*, 2007, **23**, 11684–11692.
32. M. L. Schlossman and A. M. Tikhonov, *Annu. Rev. Phys. Chem.*, 2008, **59**, 153–177.
33. M. Aratono, H. Matsubara, and T. Takiue, *J Therm Anal Calorim*, 2010, **99**, 51–55.